Supporting Information

Strongly Entangled Triplet Acyl-Alkyl Radical Pairs in Crystals of Photostable Diphenylmethyl-Adamantyl Ketones

Jin H. Park‡, Vince M. Hipwell‡, Edris A. Rivera, and Miguel A. Garcia-Garibay*

Department of Chemistry and Biochemistry, University of California, Los Angeles, California 90024-1569.

*e-mail: mgg@chem.ucla.edu

‡ These authors contributed equally

Contents: **Page Number**

General Methods. All commercially obtained reagents and solvents were used as received without further purification. Unless stated otherwise, reactions were conducted in oven-dried glassware under argon atmosphere. ^{1}H NMR spectra were recorded at 500 MHz, and ^{13}C NMR spectra were recorded at 125 MHz. All chemical shifts are reported in ppm on the δ-scale relative to TMS (δ 0.0) using residual solvent as reference ($CDCl_3$ δ 7.26 and δ 77.16 for proton and carbon, respectively, CD_3CN δ 1.94 and δ 118.26 for proton and carbon, respectively. Standard abbreviations indicating multiplicity were used as follows: s (singlet), b (broad), d (doublet), t (triplet), q (quartet), and m (multiplet). High-resolution mass spectrum data were recorded on a DART spectrometer in positive (ESI+) ion mode. UV-Vis absorption and transmission spectra were recorded on Ocean Optics spectrometer (DT-MINI-2-GS UV-VIS-NIR LightSource and USB2000+ using SpectraSuite software package). Dynamic Light Scattering (DLS) data were recorded using a Beckman-Coulter N4 Plus particle analyzer with a 10 mW helium-neon laser at 632.8 nm. The particle size was determined using the 62.6° detection angle and was calculated using the size distribution processor (SDP) analysis package provided by the manufacturer. Melting point values were recorded on a Melt-Point II® apparatus. Infrared spectra were recorded on a PerkinElmer® Spectrum Two spectrometer equipped with a universal ATR sampling accessory. Nanosecond transient absorption experiments were performed using Laser Flash Photolysis instrument from Edinburgh Instruments in conjunction with a Nd:YAG laser (Brilliant b, Quantel®) with 266-nm output, 4-6 ns pulse width and 36-40 mJ pulse energy. The optical detection is based on a pulsed Xenon arc lamp (450 W), a monochromator (TMS300, Czerny-Turner), a photomultiplier detector (Hamamatsu R928) and a digital oscilloscope (TDS3012C, 100 MHz and 1.25 GS/s from Tektronix). The laser

flash photolysis experiments were performed with 1 cm quartz flow cell mounted on a home-built sample holder that is placed at the cross-section of the laser incident beam and the probe light. Acetonitrile solutions (continuously sparged with argon) or crystalline suspensions of ketones (2.5 mg/L) were flown through the quartz cell using a peristaltic pump (Masterflex L/S) at a rate of 1.6 – 3.2 mL/min. Due to aggregation fresh samples in batches of 20 mL were made for the crystalline suspensions every 10 minutes. Time-resolved absorption maps were recorded with continuous flow of samples through the quartz cell. Data was collected at 10 nm intervals from 310 nm to 400 nm, and the spectra were constructed and smoothed with Origin software. Lifetimes at λ_{max} for end-of-pulse spectra were reproducible and doubly verified/processed with Edinburgh Instruments L900 internal software and Igor Pro software. The parameters under the detector monochromator settings are as follows: the ketones were observed at the corresponding λ_{max} in solution (320-330 nm) and in crystalline suspensions (330-340 nm), and the band width was set between 1.00 to 3.00 nm. The flash lamp settings were set with the frequency at 10 Hz, width at 40 μs, and delay at 4000 μs. The Q-switch settings were set with the frequency at 1.0 Hz, width at 20 μs, and delay between 260-300 μs.

Experimental Section:

General Synthesis of Acid Chlorides: To mitigate costs, the synthesis of several commercially available acid chlorides was performed according to literature precedent with slight modifications.[1] In a flame-dried, argon filled round-bottom flask, the corresponding carboxylic acid (1 eq) was stirred under dry DCM (15 eq) and treated with oxalyl chloride (1.1 eq). The reaction was allowed to stir for 20 minutes, then treated with dry dimethylformamide (0.01 eq). After the formation of gas ceases the reaction was allowed to react further for 2 hours. The solvents were removed under reduced pressure. The resulting liquid is then stored in a vial for the proceeding steps.

General Synthesis of ketones: Following a modified procedure by Rajca *et al.*[2], in a flame-dried, argon filled round-bottom flask, acid chloride (0.5 eq) in THF was added over 5 minutes to a 5:1 THF/hexane solution of (diphenylmethyl)lithium (2.5 eq) stirring at 0 °C. The reaction undergoes a color change from a light orange-red to a deep dark red. After 1 hour, the remaining acid chloride (0.5 eq) in THF was added over 5 minutes. The reaction was warmed to room temperature and stirred overnight. The reaction was quenched with 0.5 M HCl, extracted with diethyl ether (3 X 20 mL) and dried over Na_2SO_4. The solvents were removed under reduced pressure and the residual material was subjected to column chromatography (9:1 hexanes : acetone → 4:1 hexanes : acetone). The resulting crystalline solids were further recrystallized from ethanol (19-60% yield).

Solid-State Photochemistry:

All solid state photochemistry product analysis was conducted via irradiation with a medium-pressure Hg Hanovia lamp with a pyrex immersion well filter with a cutoff of $\lambda \leq$

290 nm and analyzed by ^{1}H NMR (500 MHz, $CDCl_3$). Samples are ground between two microscope slides which are then subjected to UV irradiation inside the lamp chamber. All solution state photochemistry product analysis was conducted in the same manner with samples dissolved in MeCN.

Compound Characterization:

1,2,2-triphenylethan-1-one (1a): Yield 65%; m.p. 66.0-67.0 °C; IR (neat) ν_{max} = 3085, 3060, 3026, 2924, 2854, 1684, 1596, 1495, 1447, 1207, 1007, 745, 696 cm^{-1}; UV-Vis λ_{max} = 245-250, 270-275 nm; R_f = 0.42 (19:1 hexanes : ethyl acetate); ^{1}H NMR (500 MHz, $CDCl_3$) δ 8.00 (m, 2H), 7.51 (m, 1H), 7.40 (m, 2H), 7.34-7.23 (m, 10H), 6.04 (s, 1H); ^{13}C{^{1}H} NMR (125 MHz, $CDCl_3$) δ 198.2, 139.1, 136.8, 133.1, 129.2, 129.0, 128.7, 128.6, 127.2, 59.4. HRMS (DART) calcd. for $[C_{20}H_{16}O+H]^+$ 273.1274, found 273.1262.

3-((3r,5r,7r)-adamantan-1-yl)-1,1-diphenylpropan-2-one (1b): Yield 40%; m.p. 102.3-103.2 °C; IR (neat) ν_{max} = 3027, 2903, 2841, 1707, 1495, 1450, 1083 cm^{-1}; UV-Vis λ_{max} = 255-260, 290-310 nm; R_f = 0.44 (19:1 hexanes : ethyl acetate); ^{1}H NMR (500 MHz, $CDCl_3$) δ 7.32 (m, 4H), 7.24 (m, 6H), 5.08 (s, 1H), 2.28 (s, 2H), 1.94 (s, 3H), 1.65 (m, 12H); ^{13}C{^{1}H} NMR (125 MHz, $CDCl_3$) δ 207.8, 138.4, 129.1, 128.6, 127.1, 66.2, 55.9, 42.4, 36.8, 33.9, 28.6; HRMS (DART) calcd. for $[C_{25}H_{28}O+H]^+$ 345.2213, found 345.2197.

1-((1r,3r,5r,7r)-adamantan-2-yl)-2,2-diphenylethan-1-one (1c): Yield 19%; m.p. 89.4-89.7 °C; IR (neat) ν_{max} = 3061, 2905, 2848, 1700, 1495, 1447, 1093, 1028 cm^{-1}; UV-Vis λ_{max} = 255-260, 295-305 nm; R_f = 0.44 (19:1 hexanes : ethyl acetate); ^{1}H NMR (500 MHz, $CDCl_3$) δ 7.30 (m, 5H), 7.24 (m, 5H), 5.40 (s, 1H), 2.75 (s, 1H), 2.39 (s, 2H); 1.82 (m, 10H), 1.55 (m, 2H); ^{13}C{^{1}H} NMR (125 MHz, $CDCl_3$) δ 210.7, 139.1, 128.9, 128.6, 127.0, 60.6, 57.1, 38.5,

37.3, 33.1, 29.6, 27.7, 27.5; HRMS (DART) calcd. for $[C_{24}H_{26}O+H]^+$ 331.2056, found 331.2041.

1-((3r,5r,7r)-adamantan-1-yl)-2,2-diphenylethan-1-one (1d): Yield 55%; m.p. 104.4-105.0 °C; IR (neat) ν_{max} = 3051, 2910, 2848, 1700, 1494, 1445, 1348, 1021 cm^{-1};UV-Vis λ_{max} = 260-265, 295-305 nm; R_f = 0.41 (19:1 hexanes : ethyl acetate); ^1H NMR (500 MHz, $CDCl_3$) δ 7.28 (m, 4H), 7.22 (m, 6H), 5.62 (s, 1H), 2.02 (s, 3H), 1.83 (m, 6H) 1.74-1.64 (m, 6H); $^{13}C\{^1H\}$ NMR (125 MHz, $CDCl_3$) δ 212.5, 139.4, 128.9, 128.5, 126.9, 56.7, 47.9, 38.2, 36.5, 27.9. HRMS (DART) calcd. for $[C_{24}H_{26}O+H]^+$ 331.2056, found 331.2065.

Spectral data (^{1}H NMR, ^{13}C NMR, UV-Vis)

Figure S1. ^{1}H NMR (500 MHz, $CDCl_3$) of 1a.

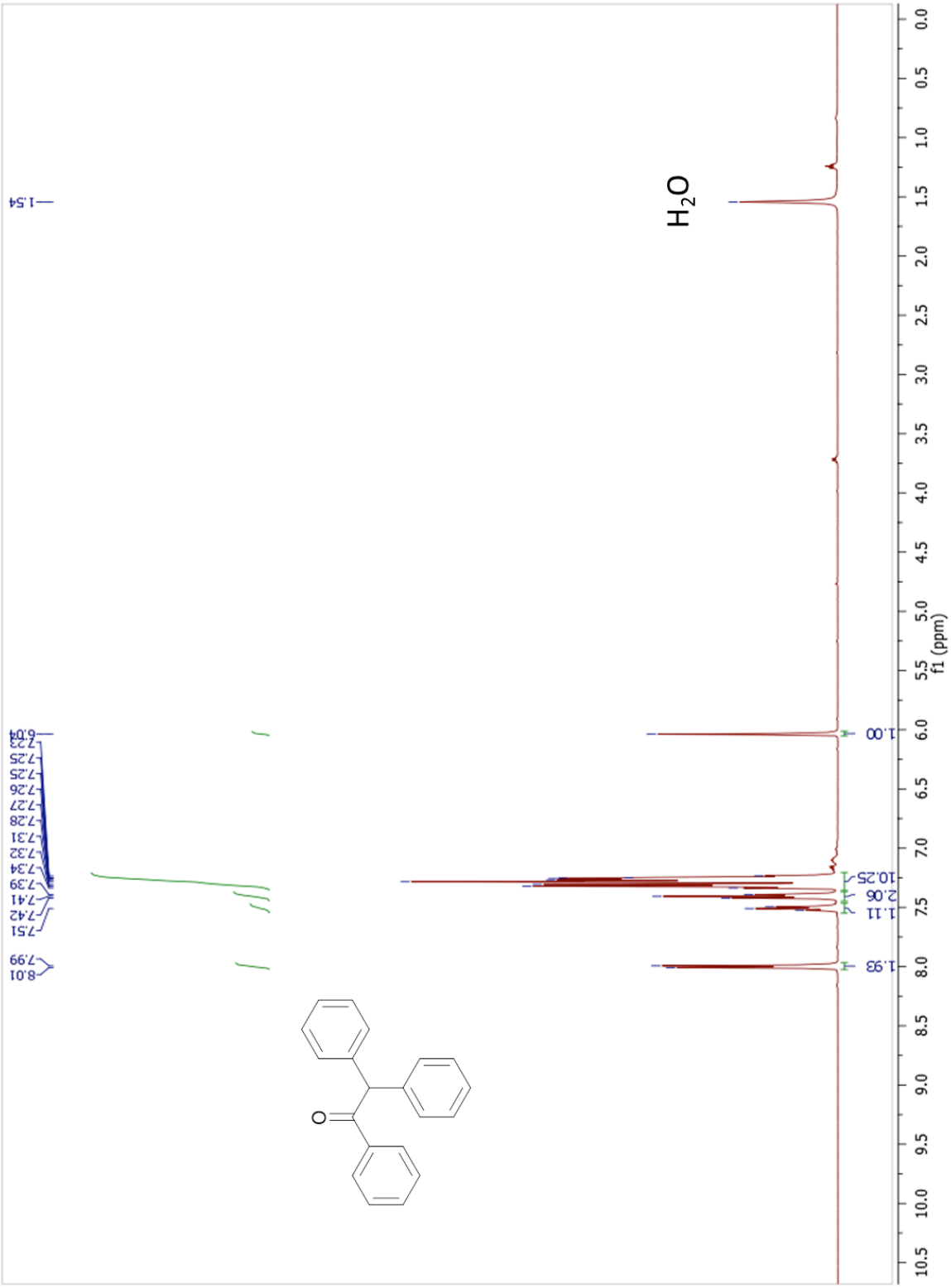

Figure S2. $^{13}C\{^{1}H\}$ NMR (125 MHz, $CDCl_3$) of 1a.

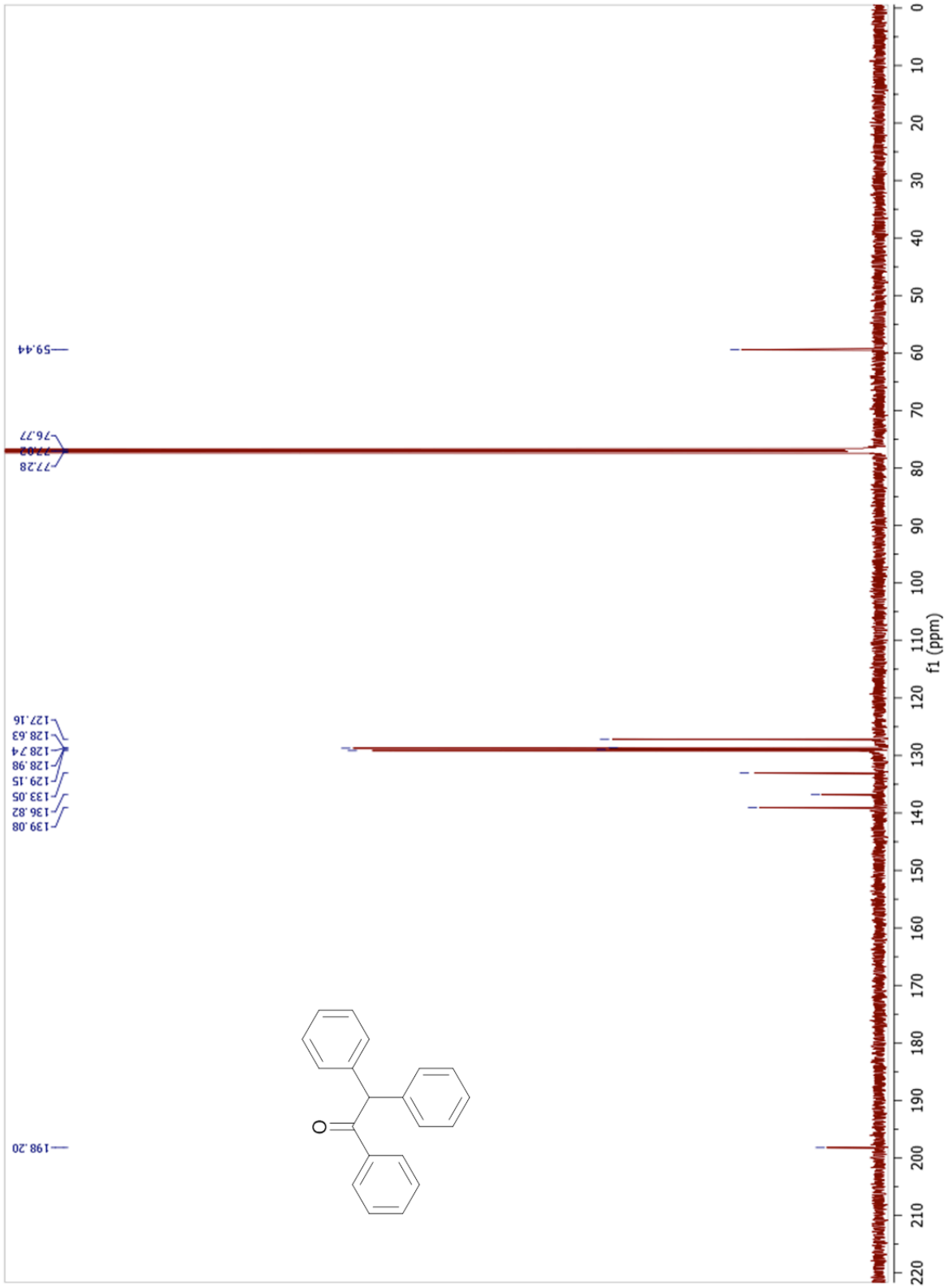

Figure S3. ^{1}H NMR (500 MHz, $CDCl_3$) of 1b.

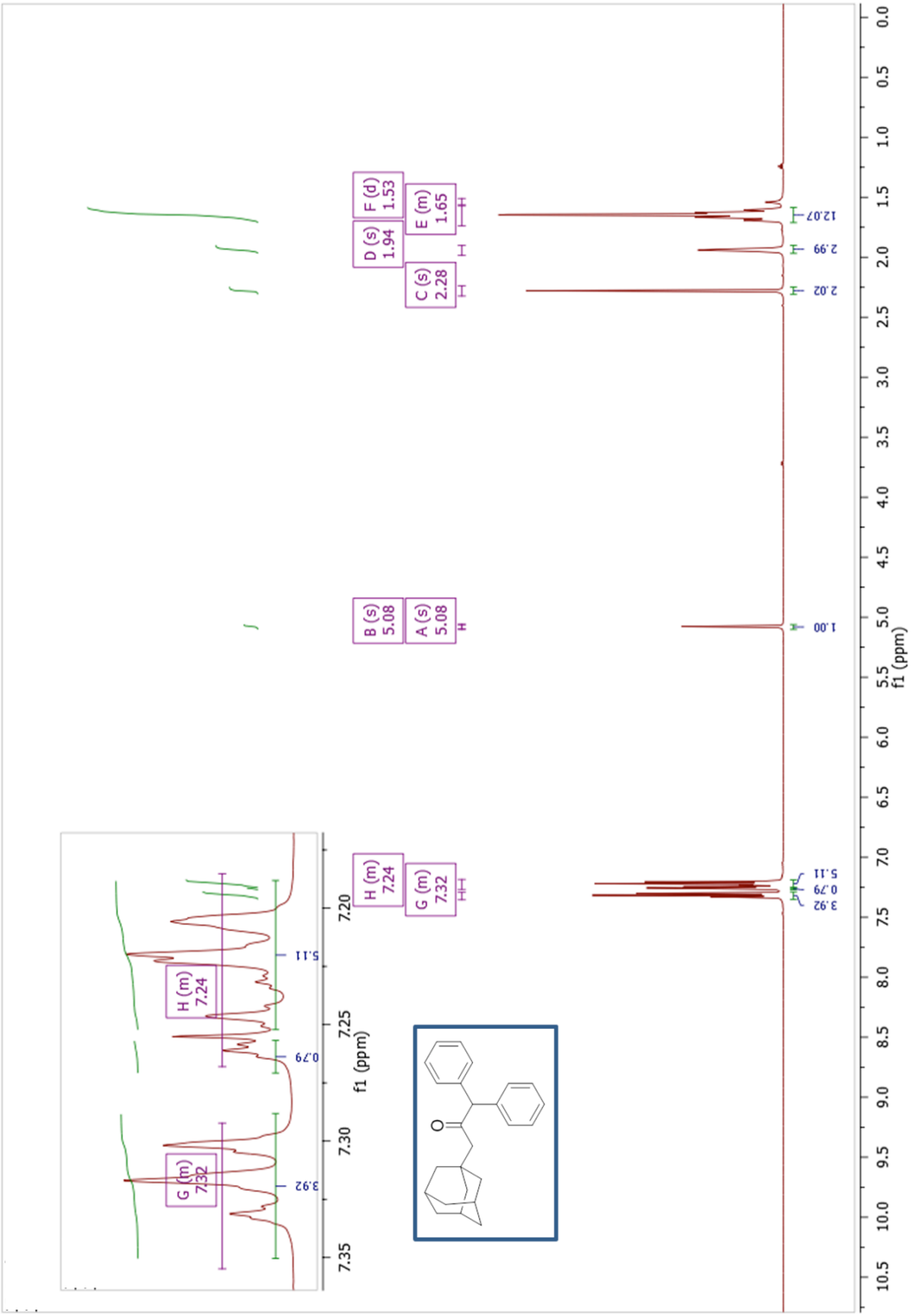

Figure S4. $^{13}C\{^{1}H\}$ NMR (125 MHz, $CDCl_3$) of 1b.

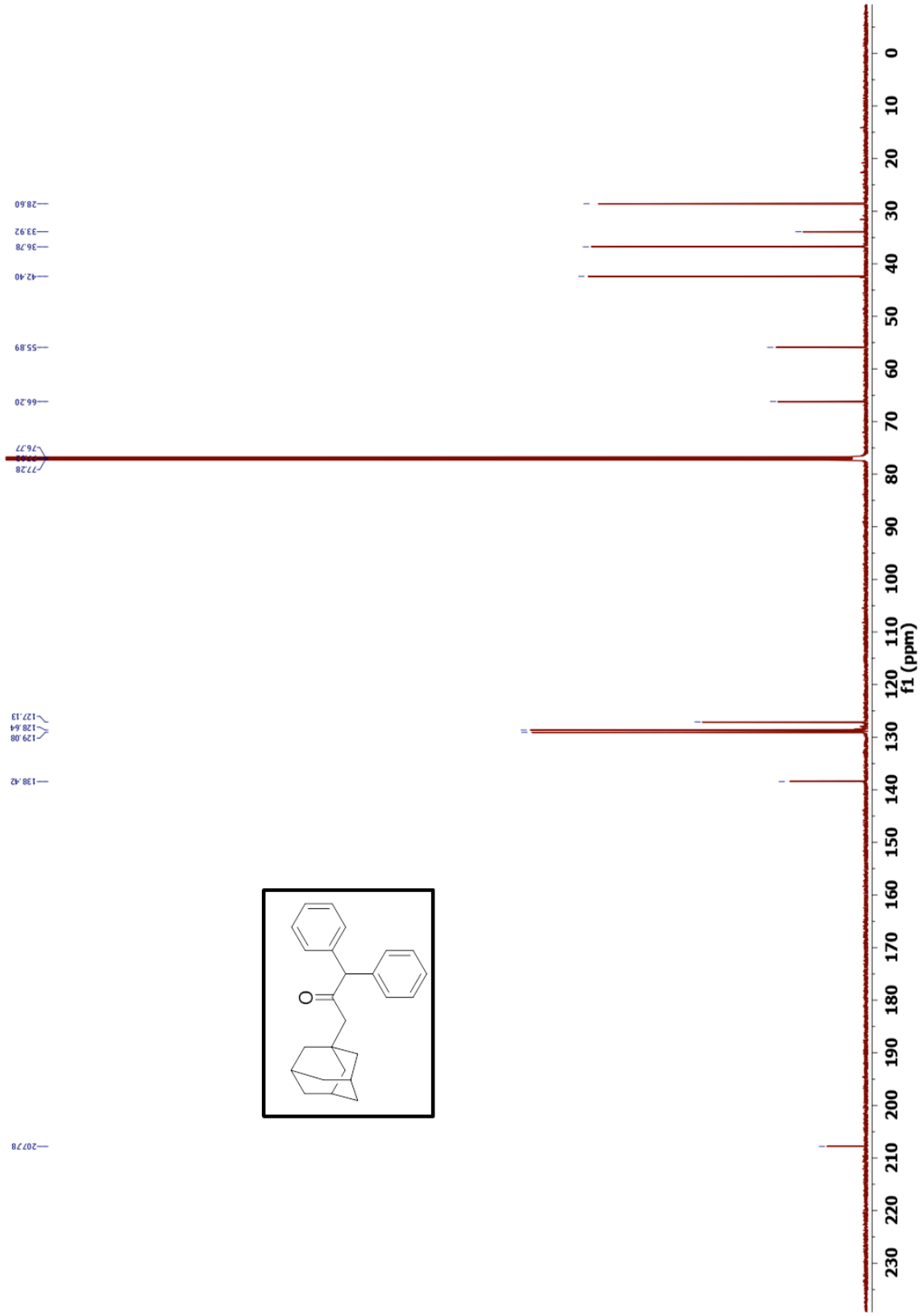

Figure S5. ^{1}H NMR (500 MHz, $CDCl_3$) of 1c.

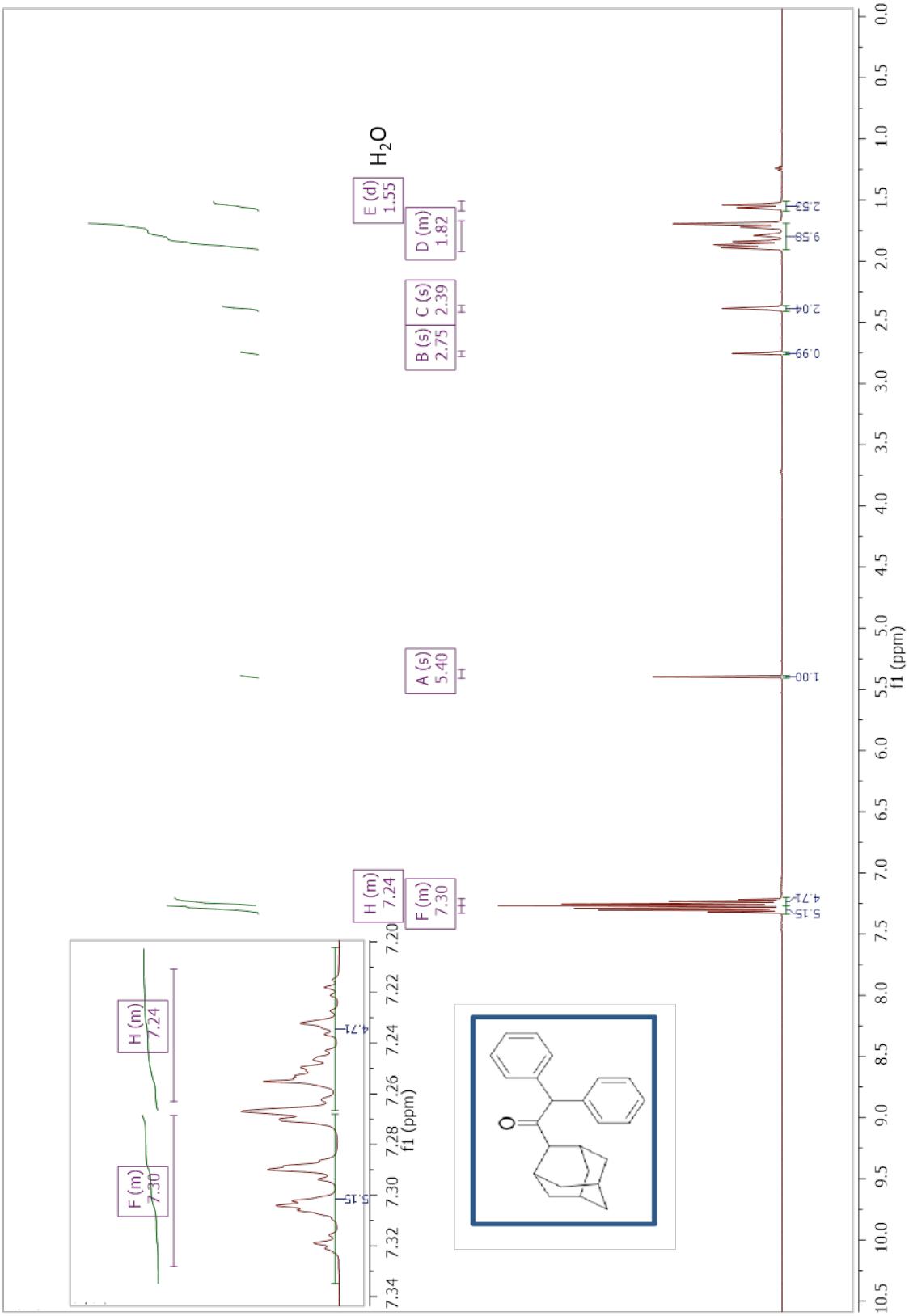

Figure S6. $^{13}C\{^{1}H\}$ NMR (125 MHz, $CDCl_3$) of 1c.

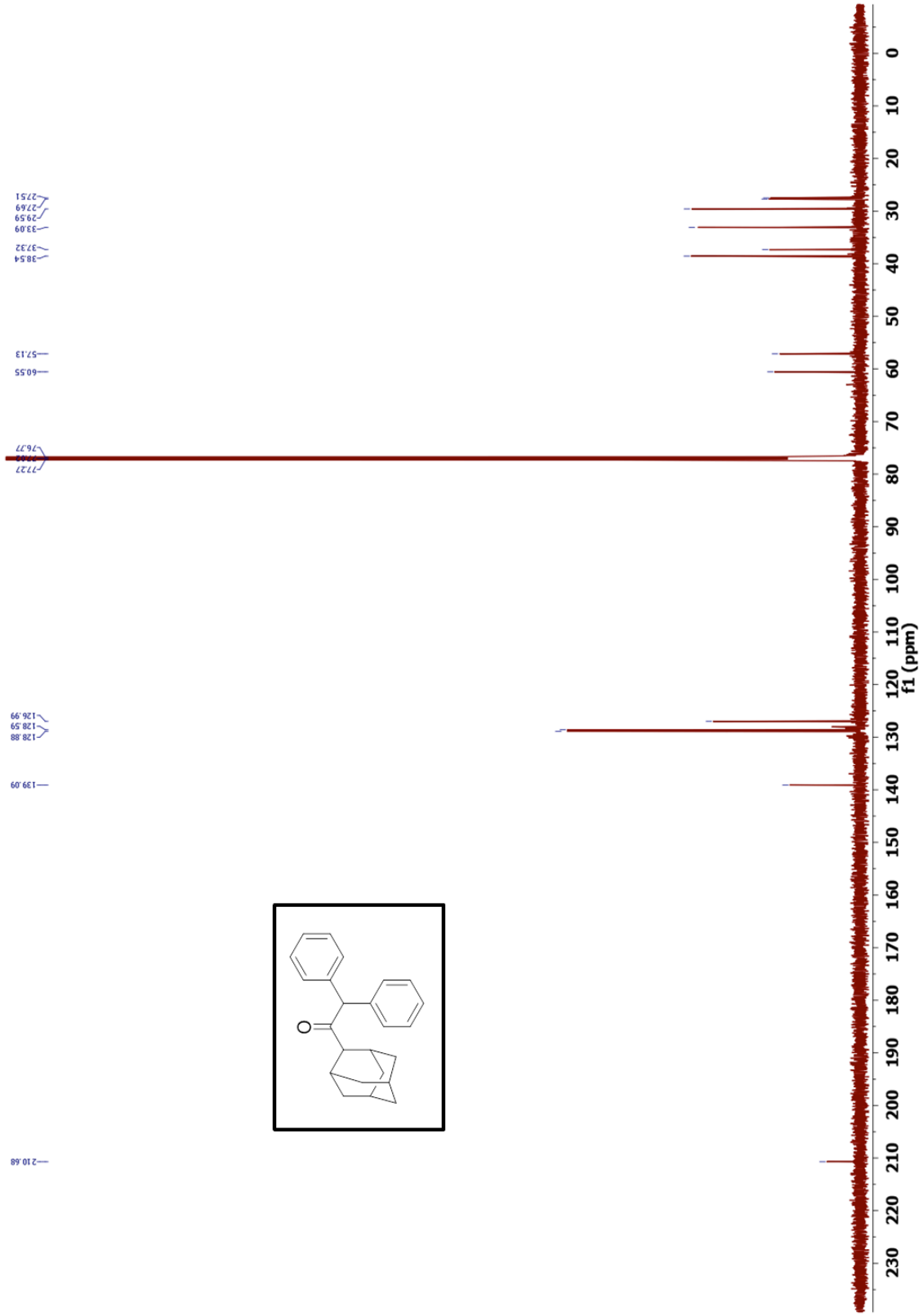

Figure S7. ^{1}H NMR (500 MHz, $CDCl_3$) of 1d.

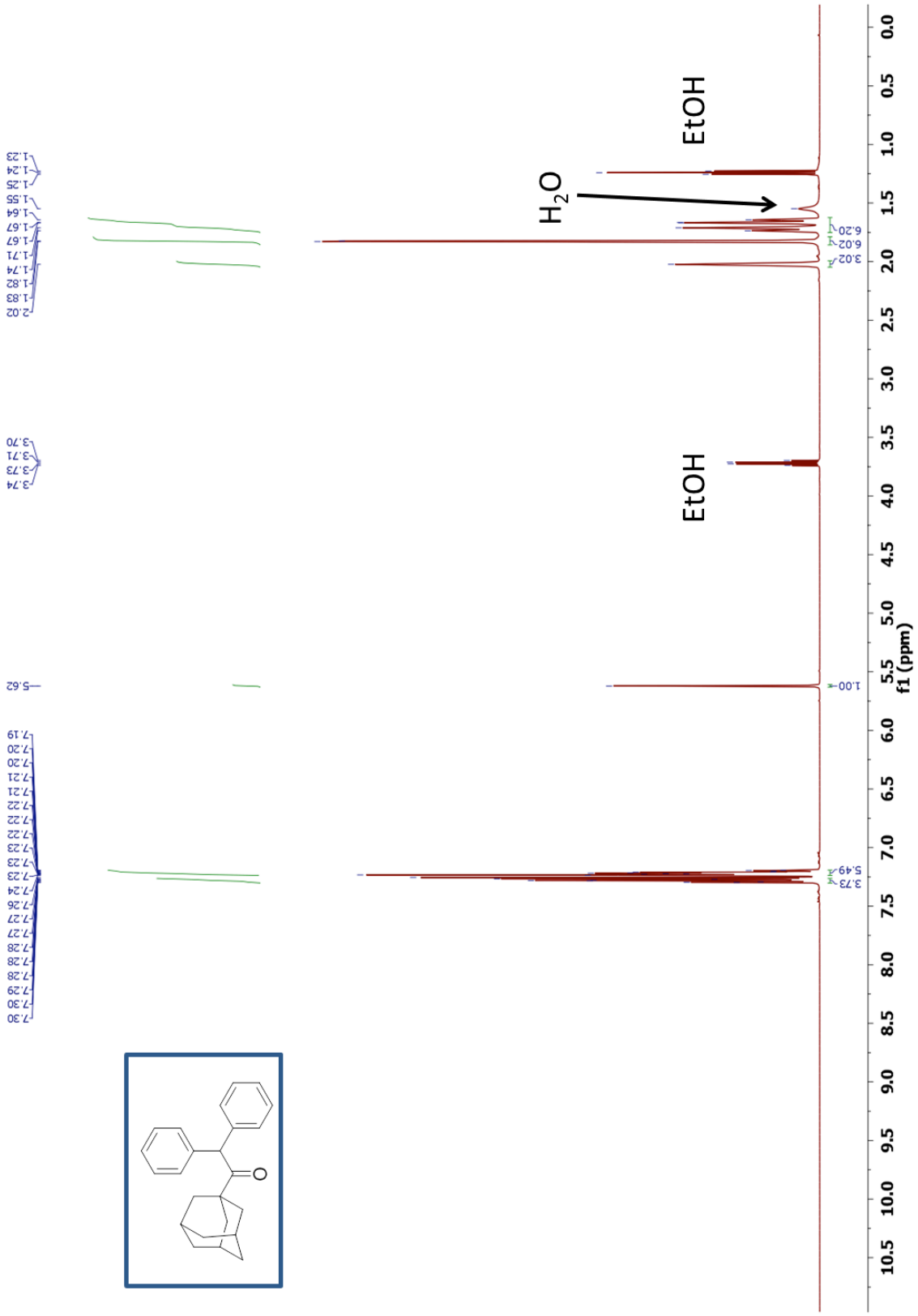

Figure S8. $^{13}C\{^{1}H\}$ NMR (125 MHz, $CDCl_3$) of 1d.

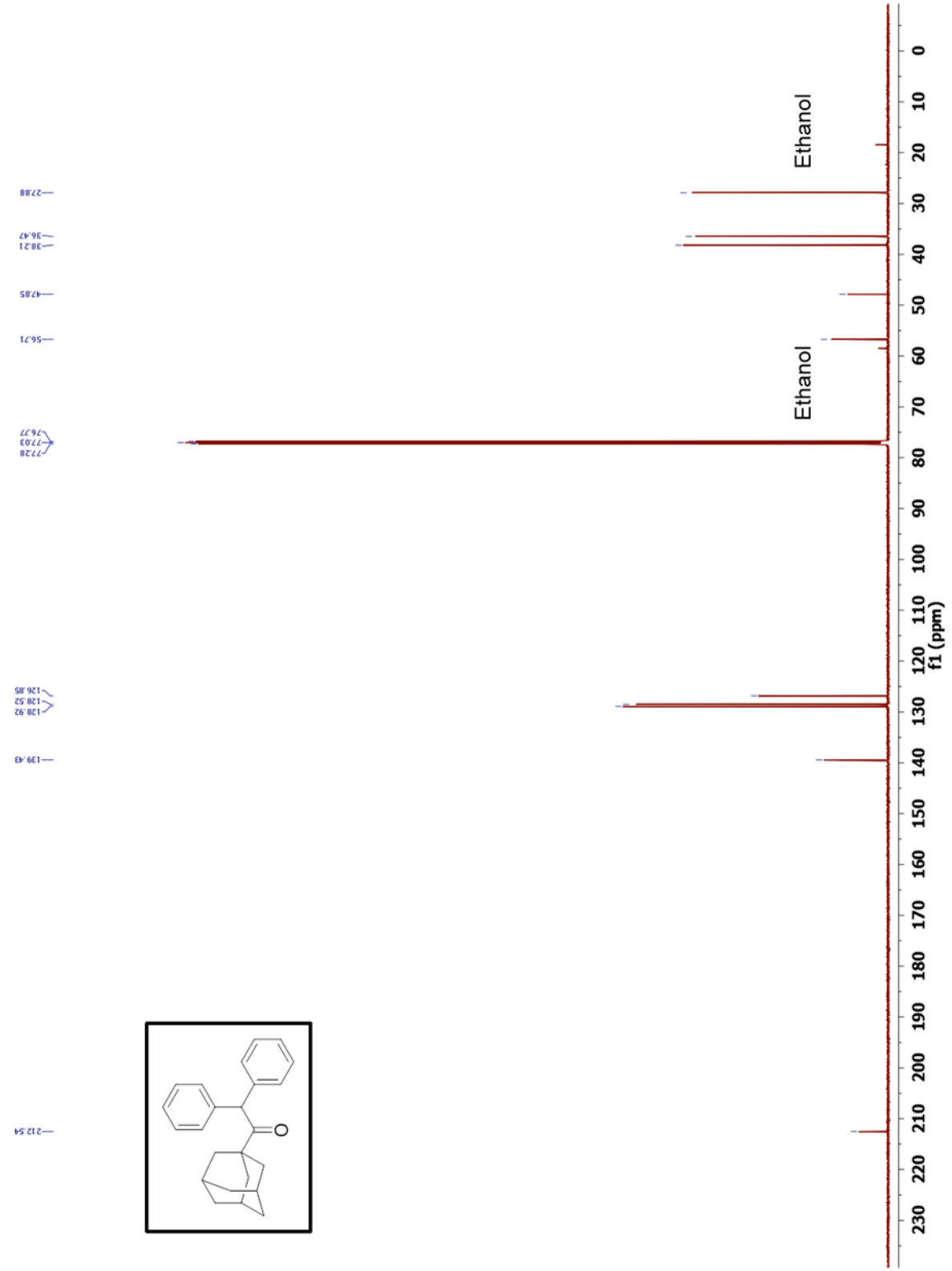

Figure S9. UV-Vis Spectra of 1a.

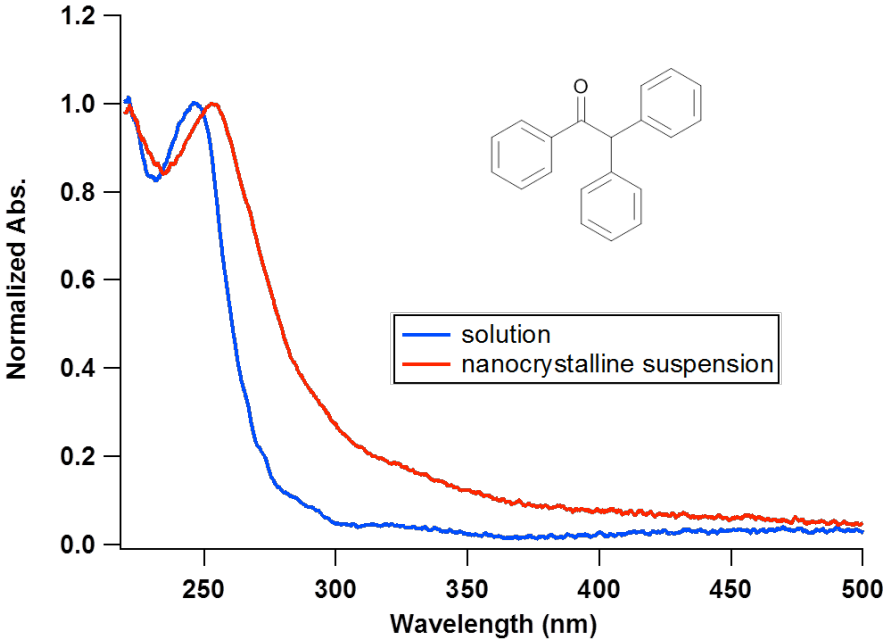

Figure S10. UV-Vis Spectra of 1b.

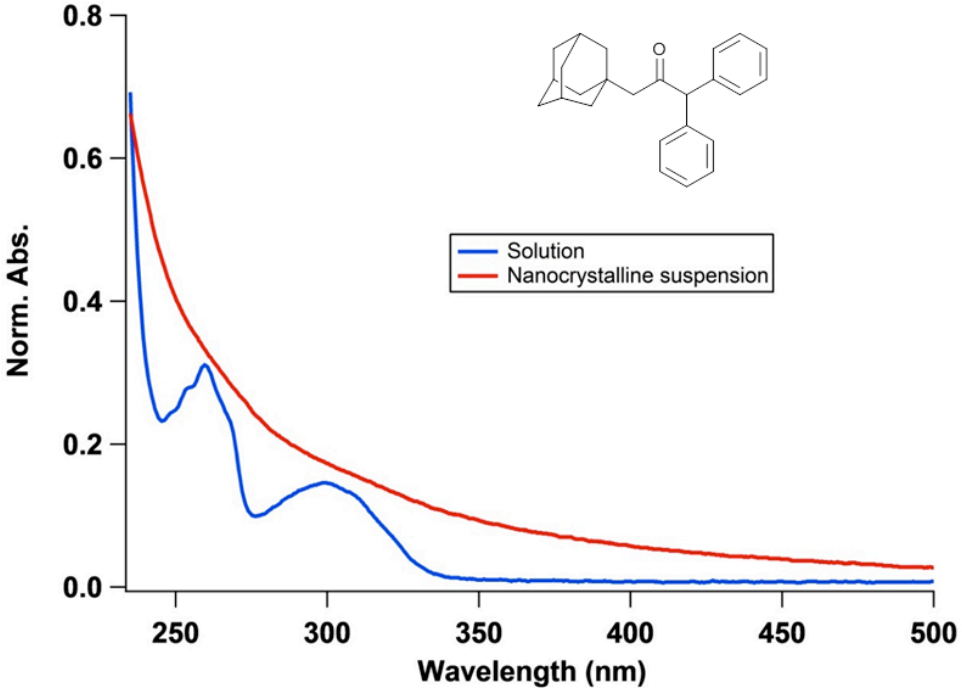

Figure S11. UV-Vis Spectra of 1c.

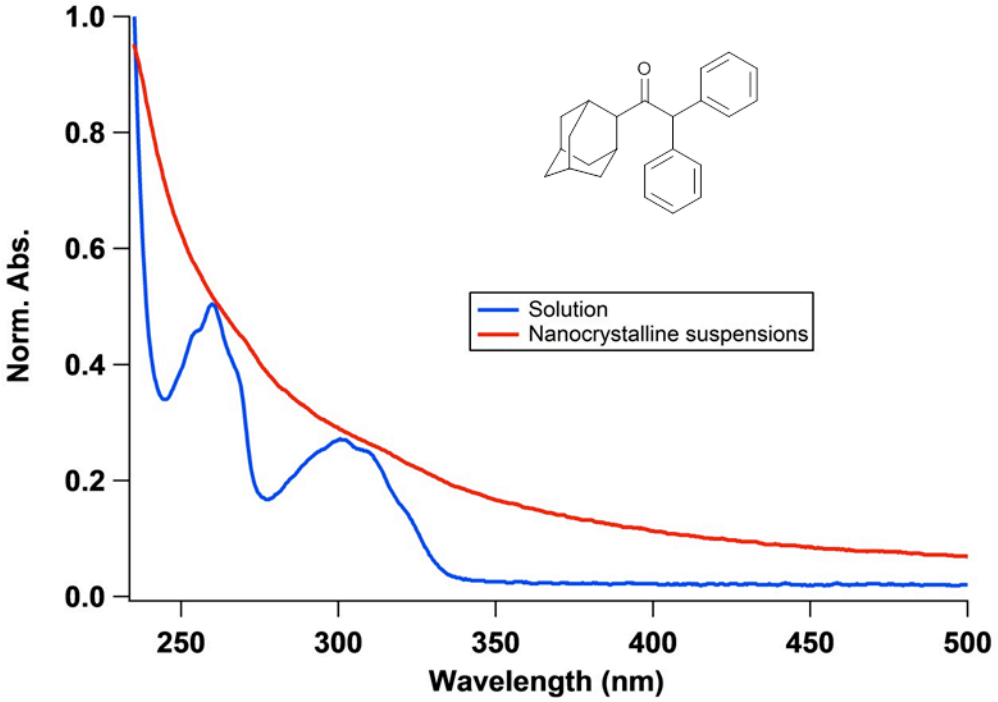

Figure S12. UV-Vis Spectra of 1d.

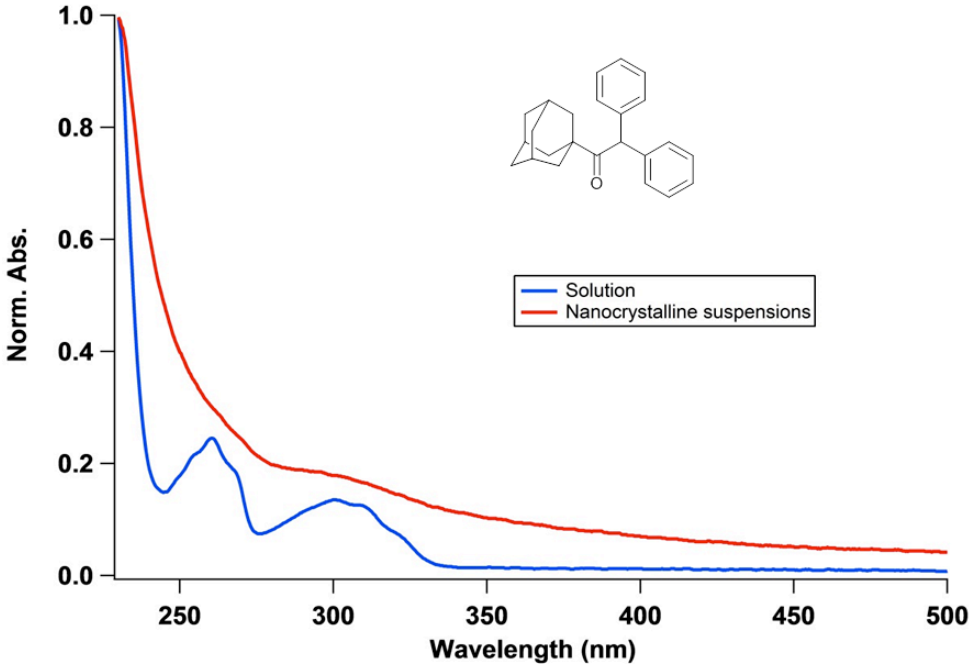

Figure S13. PXRD Data for 1a.

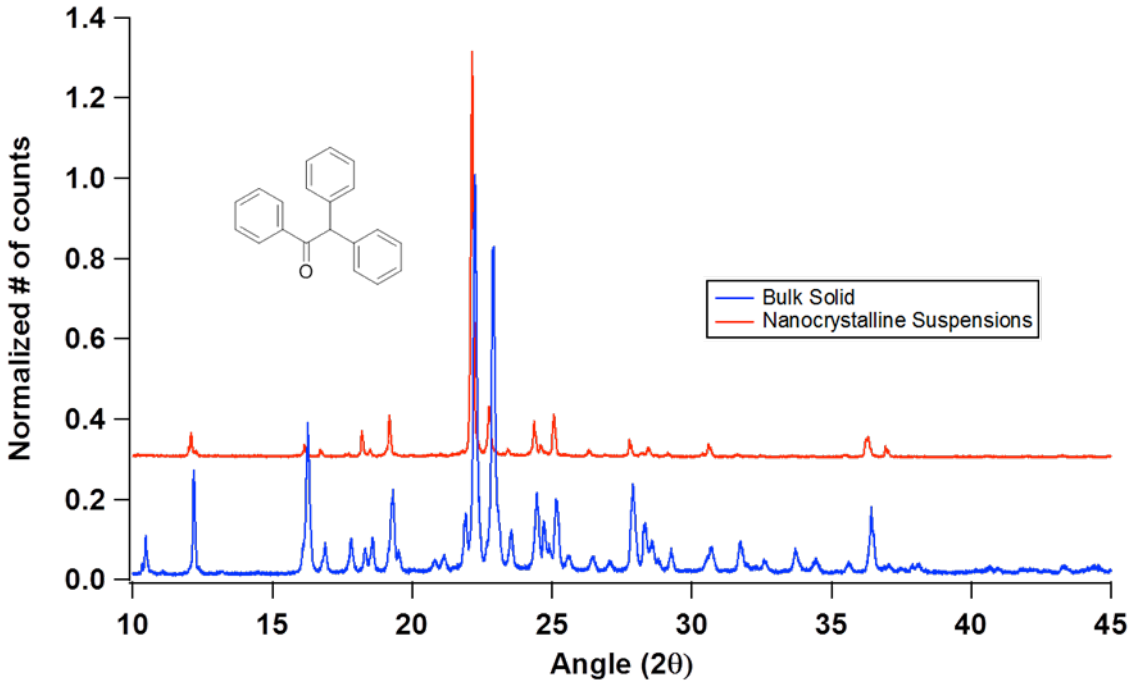

Figure S14. PXRD Data for 1b.

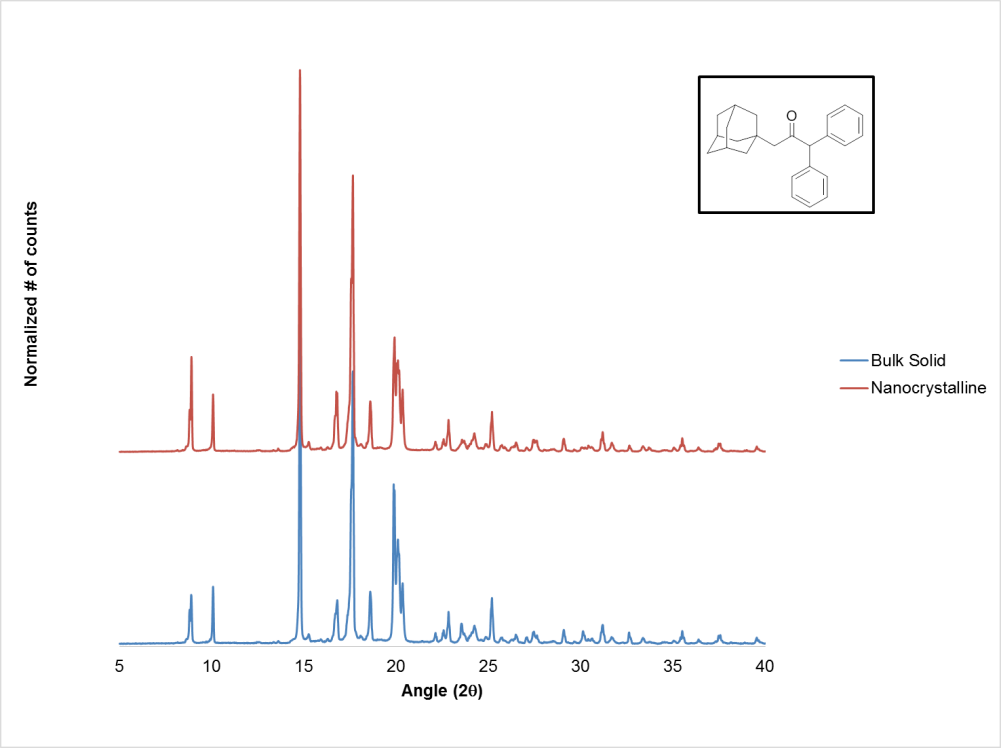

Figure S15. PXRD Data for 1c.

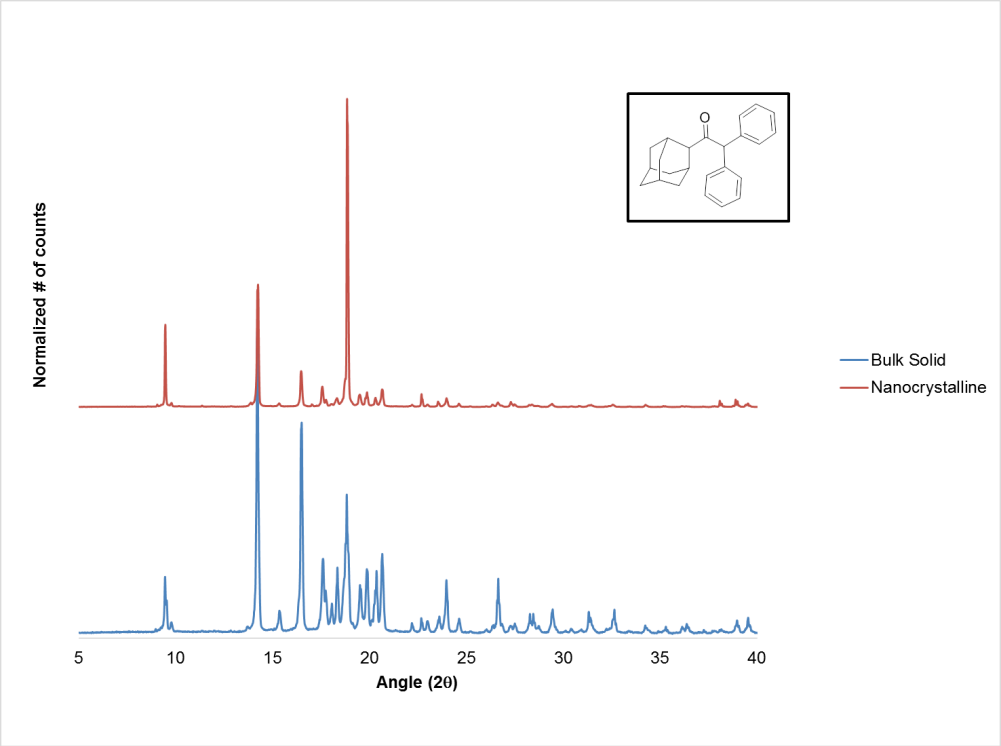

Figure S16. PXRD Data for 1d.

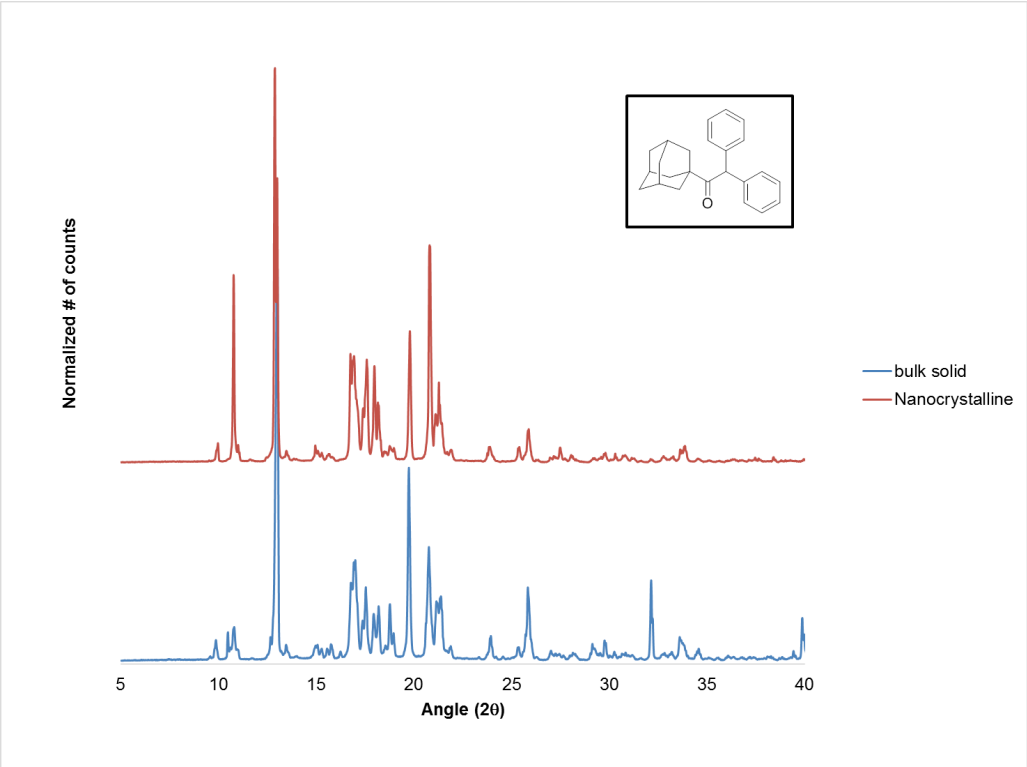

Figure S17. ^{1}H NMR Photoproduct Analysis for 1a.

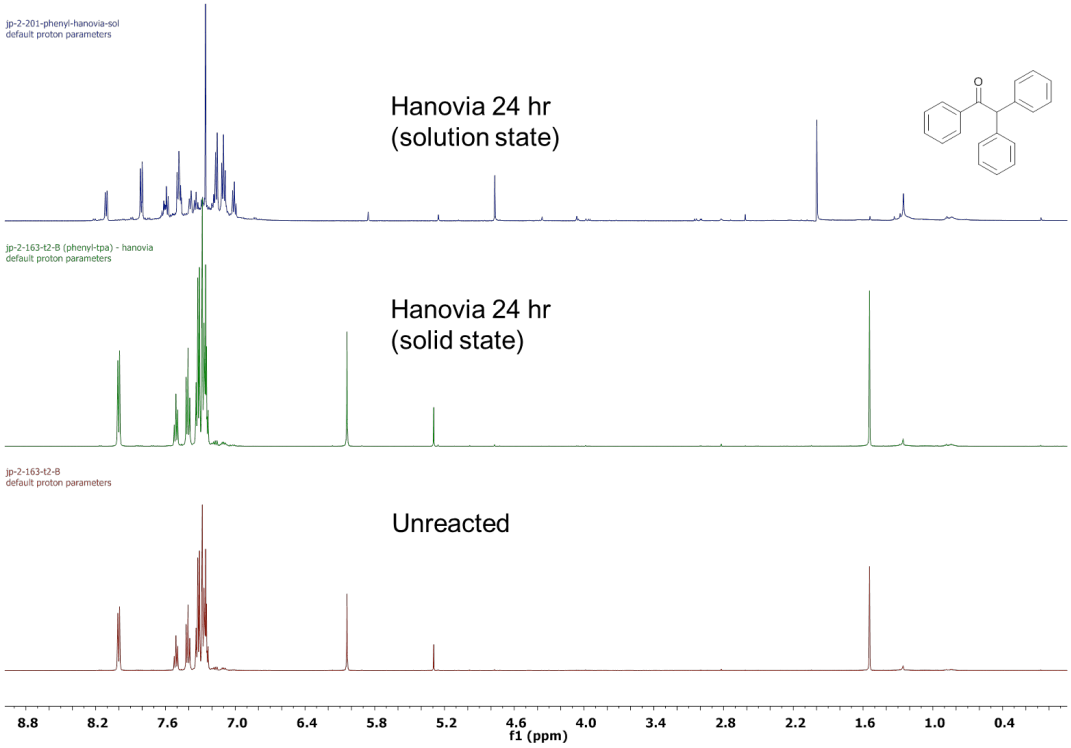

Figure S18. ^{1}H NMR Photoproduct Analysis for 1b.

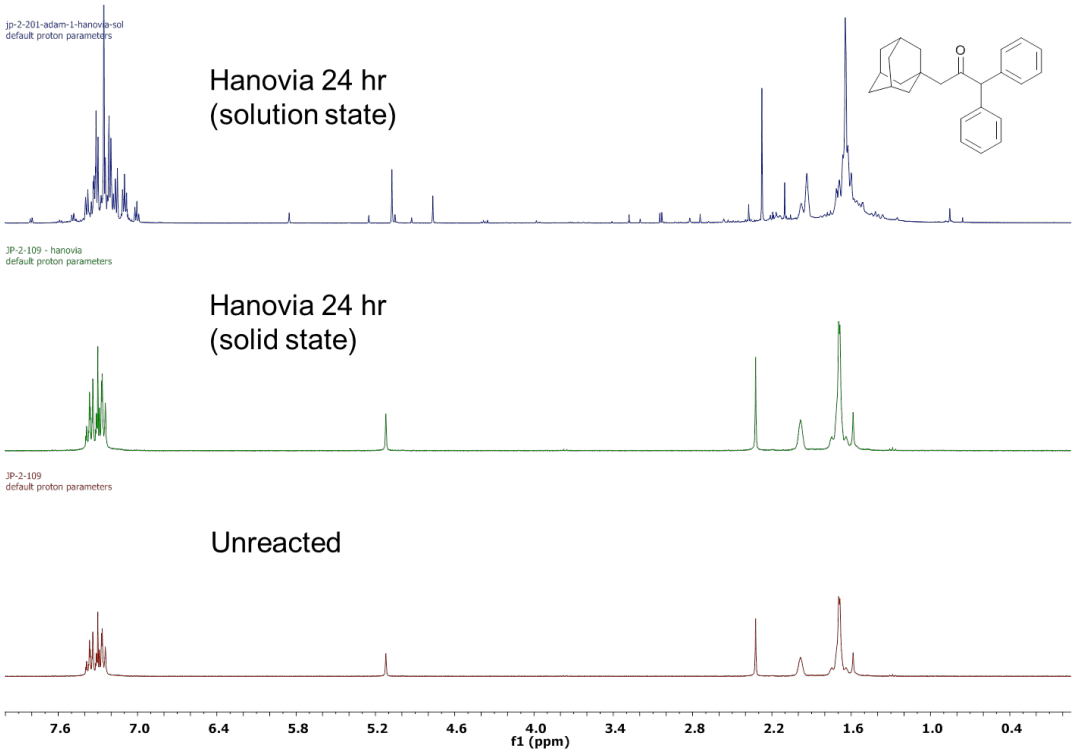

Figure S19. ^{1}H NMR Photoproduct Analysis for 1c.

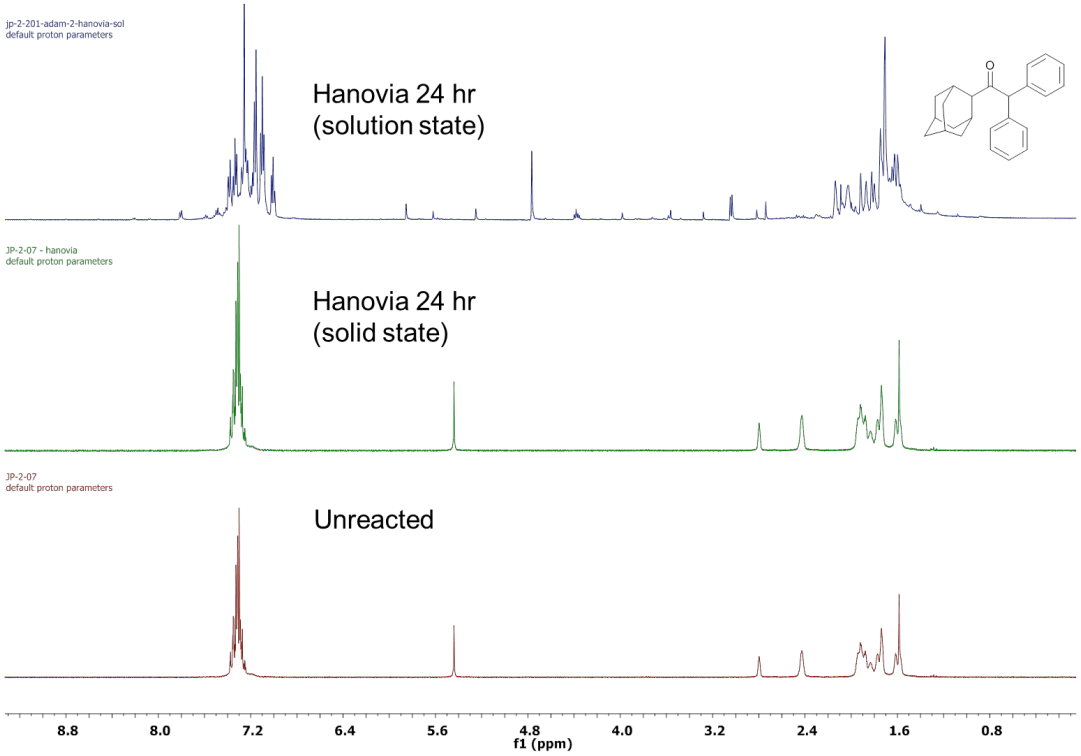

Figure S20. ^{1}H NMR Photoproduct Analysis for 1d.

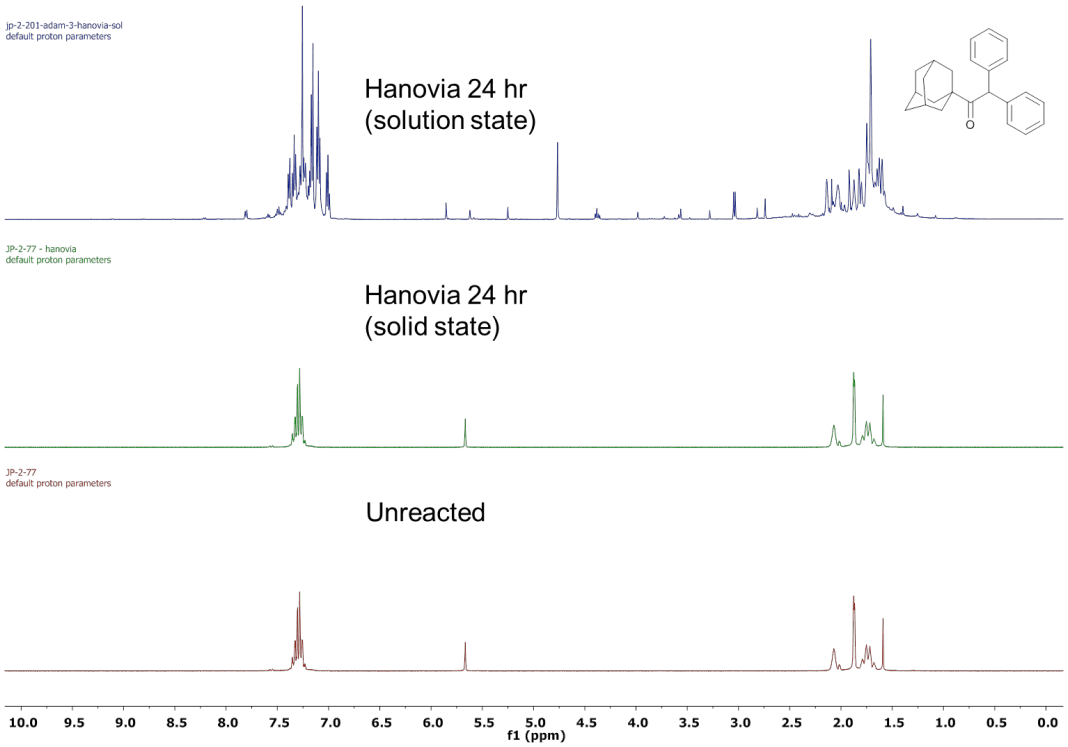

Figure S21. Transient Absorption Spectrum of 1a in MeCN Solution.

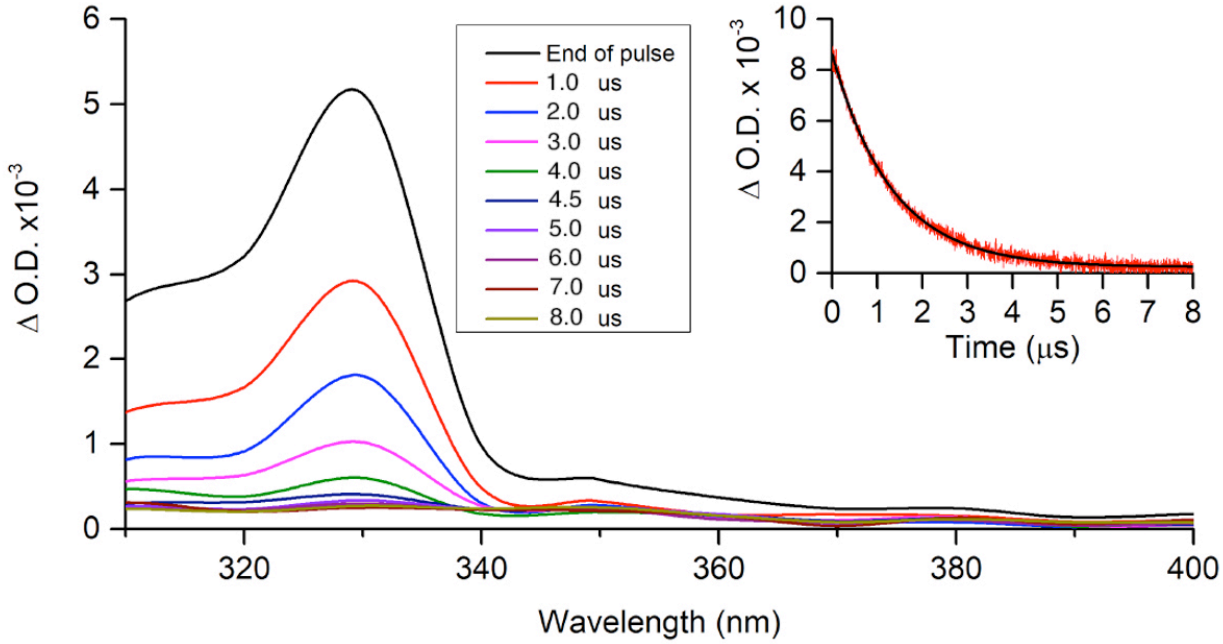

Figure S22. Transient Absorption Spectrum of 1b in MeCN Solution.

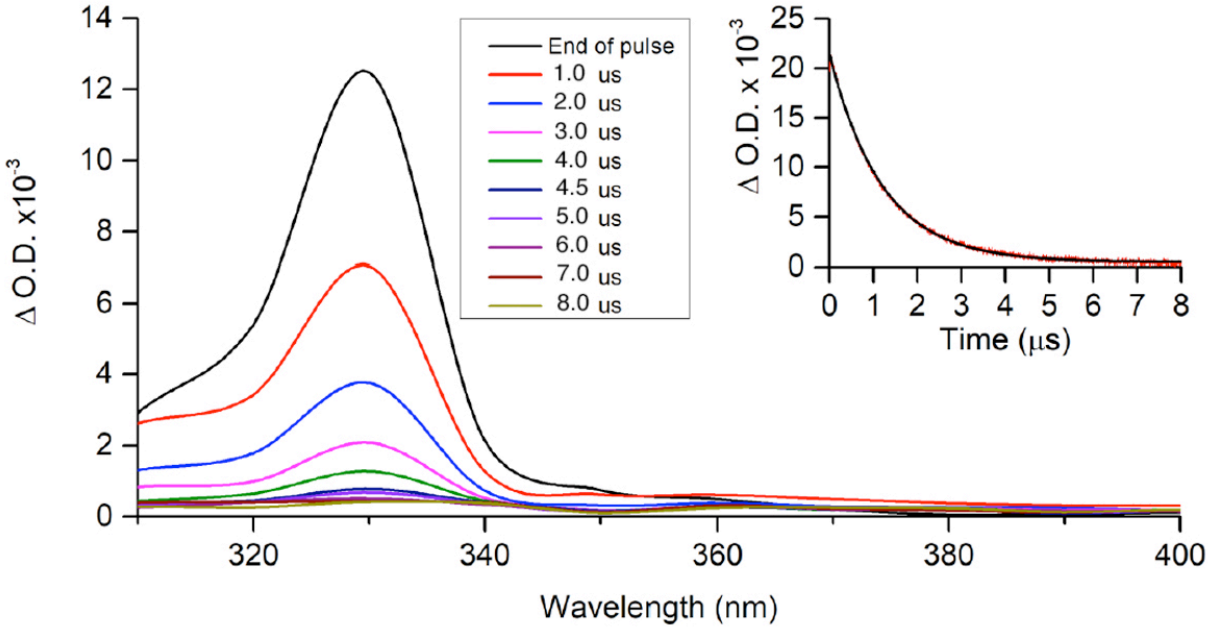

Figure S23. Transient Absorption Spectrum of 1c in MeCN Solution.

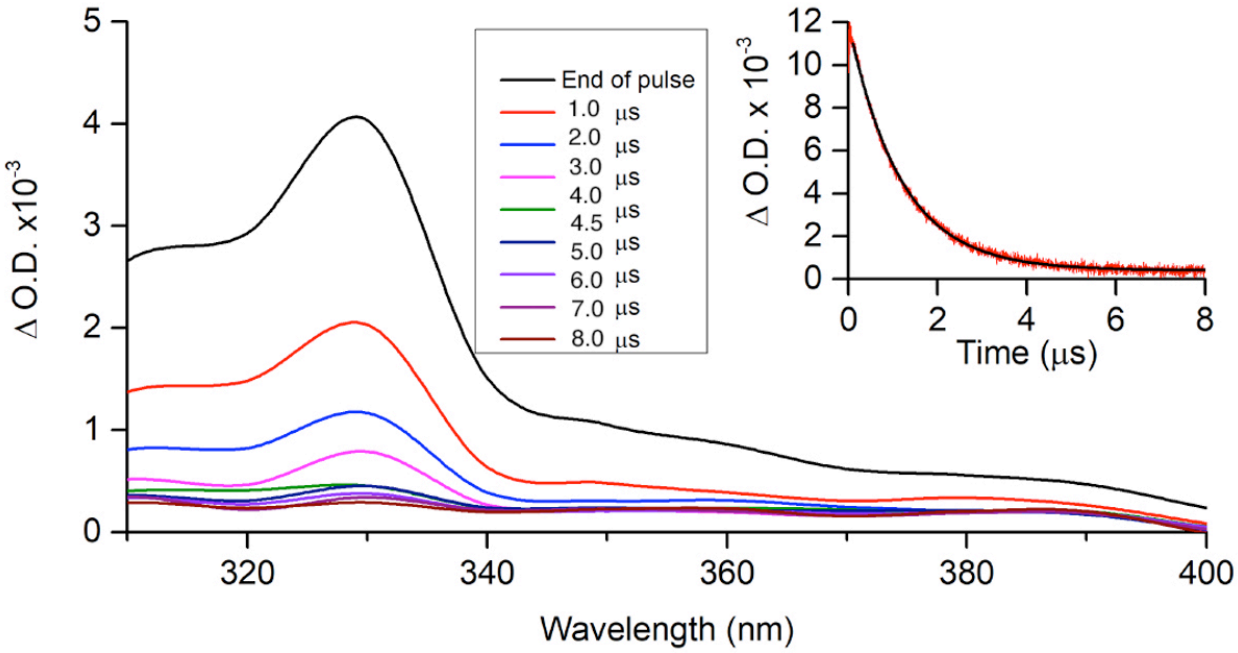

Figure S24. Transient Absorption Spectrum of 1d in MeCN Solution.

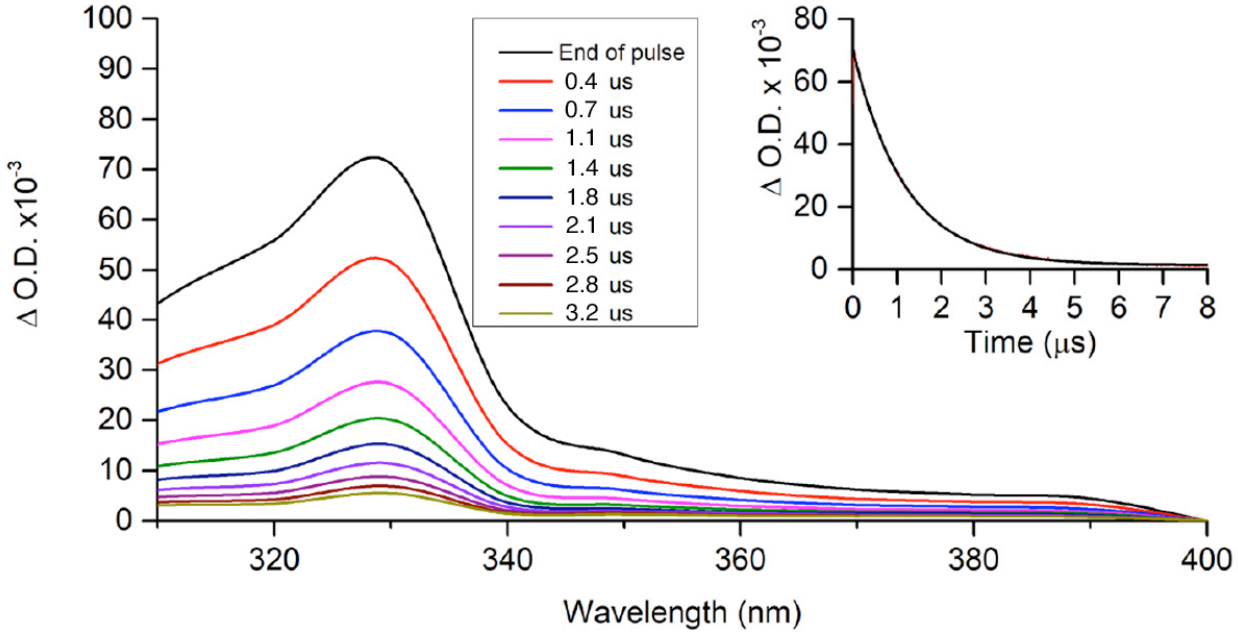

Figure S25. Transient Absorption Spectrum of 1a in Nanocrystalline Suspension.

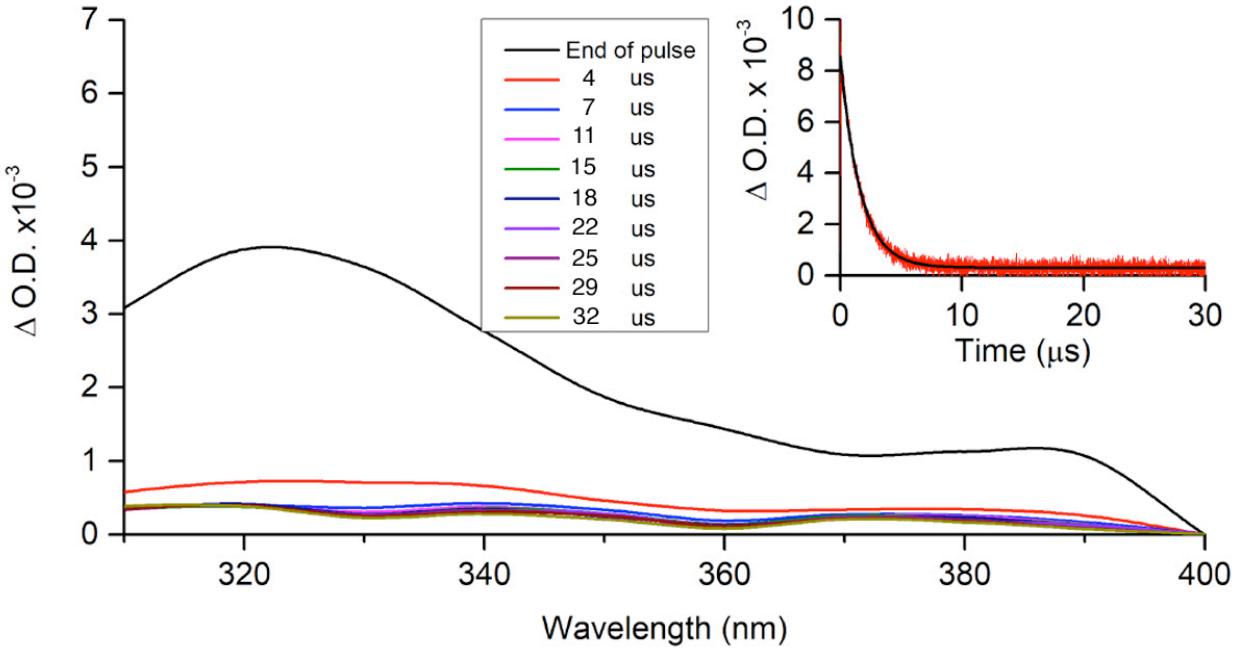

Figure S26. Transient Absorption Spectrum of 1b in Nanocrystalline Suspension.

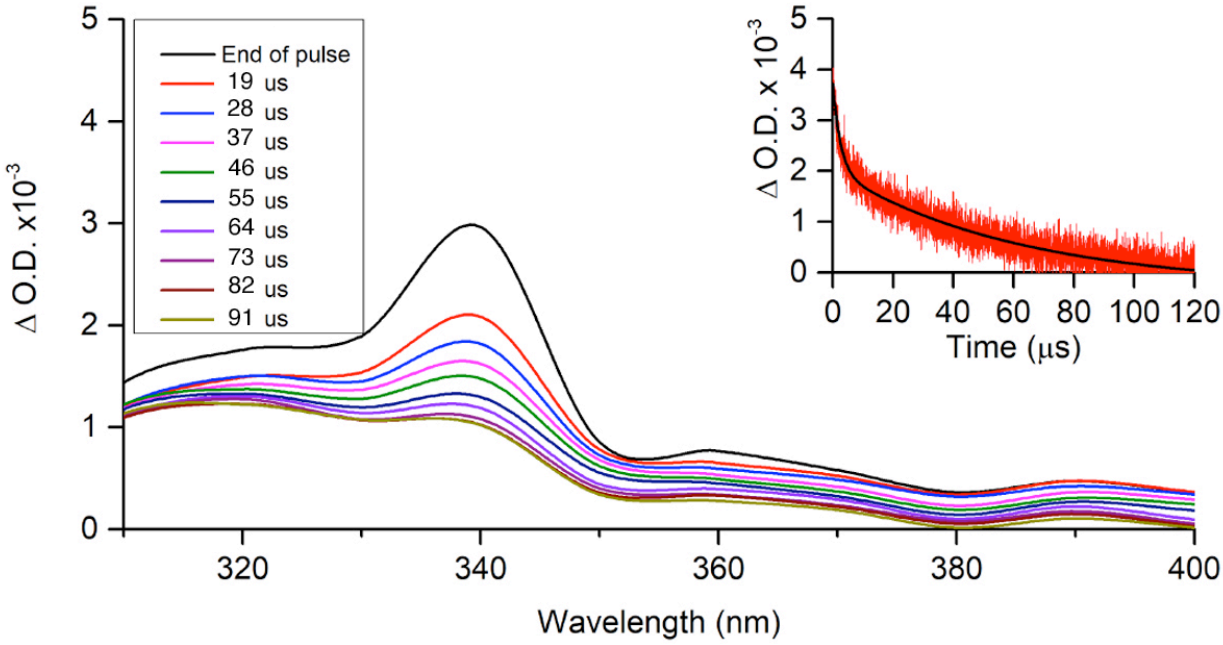

Figure S27. Transient Absorption Spectrum of 1c in Nanocrystalline Suspension.

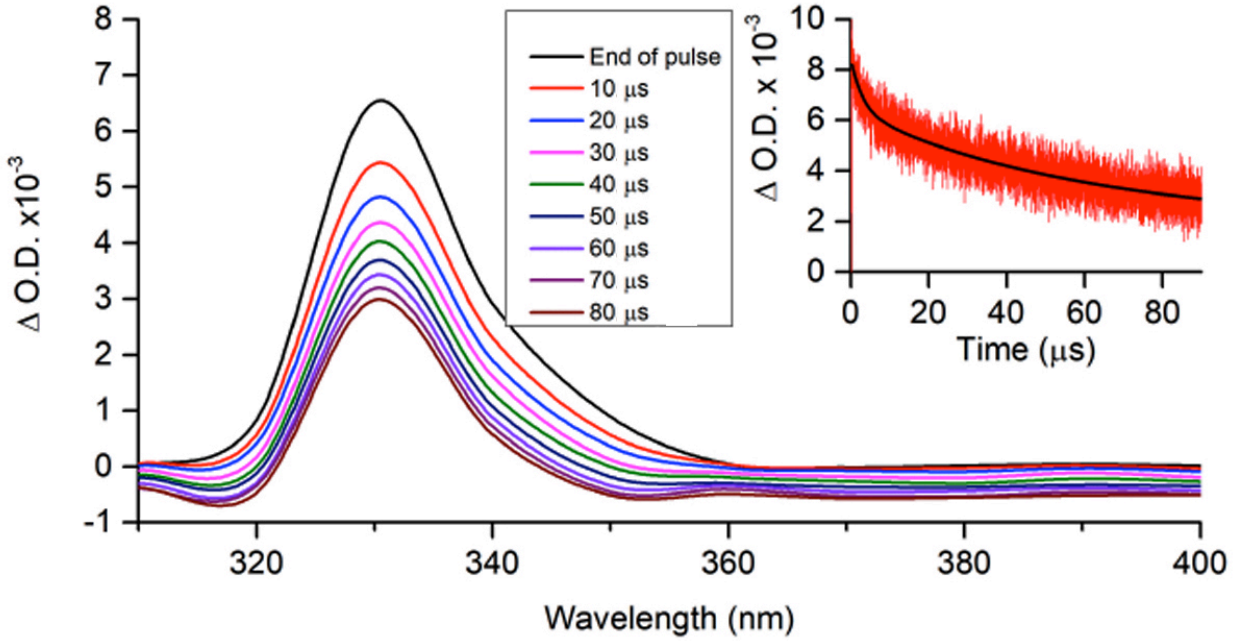

Figure S28. Transient Absorption Spectrum of 1d in Nanocrystalline Suspension.

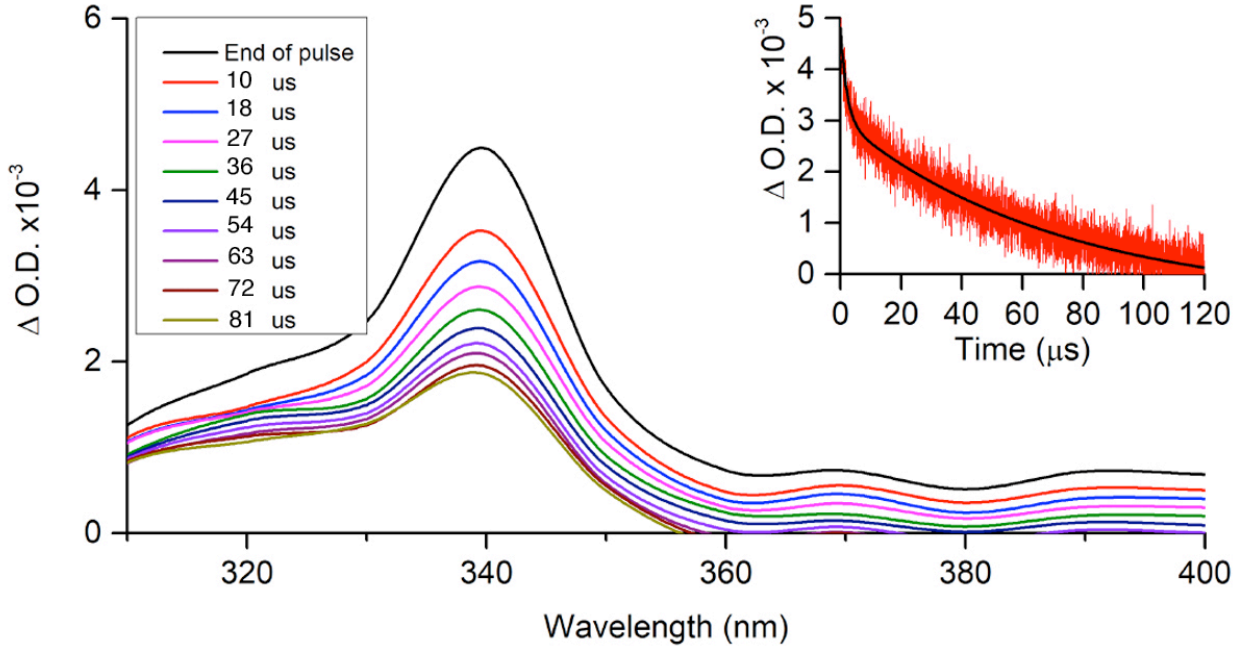

Figure S29. Dynamic Light Scattering Data for Nanocrystalline Suspension of 1a.

Unimodal Results Summary

Rept#.	Mean (nm)	Std.Dev (nm)	Baseline Error	P.I.	Counts/s	Diff.Coef (m^2/s)	Overflow
Rept.1	150.7	68.8	0.03%	0.628	1.84e+05	3.00e-12	0
Rept.2	153.8	70.3	0.02%	0.635	1.97e+05	2.94e-12	0
Rept.3	174.2	75.8	0.02%	-0.390	2.08e+05	2.60e-12	0
Average	159.6	71.63		0.291			

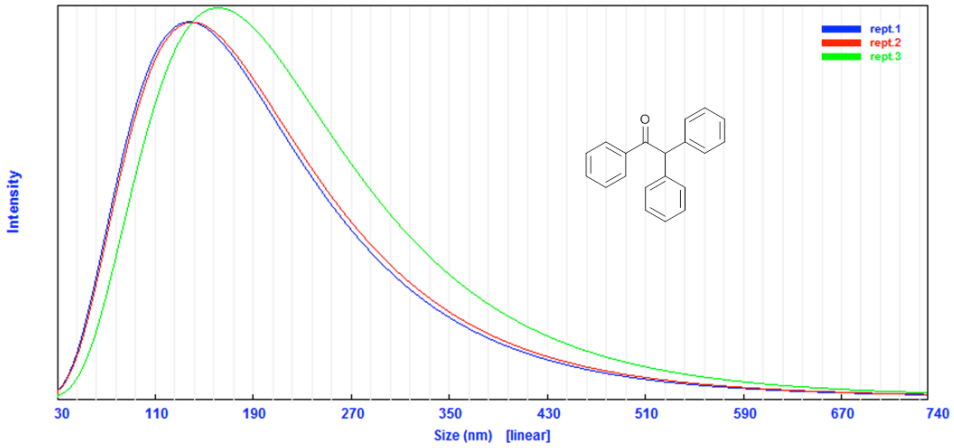

Figure S30. Dynamic Light Scattering Data for Nanocrystalline Suspension of 1b.

Unimodal Results Summary

Rept#.	Mean (nm)	Std.Dev (nm)	Baseline Error	P.I.	Counts/s	Diff.Coef (m^2/s)	Overflow
Rept.1	261.4	107.1	0.00%	0.256	4.98e+05	1.73e-12	0
Rept.2	271.9	105.8	0.01%	0.192	4.97e+05	1.66e-12	0
Rept.3	270.5	114.0	0.00%	0.308	4.92e+05	1.67e-12	0
Average	267.9	108.98		0.252			

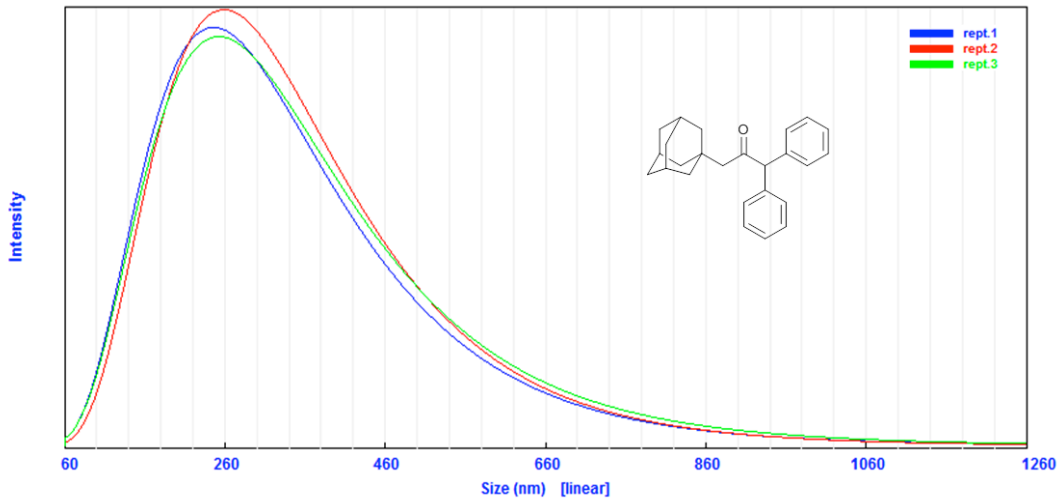

Figure S31. Dynamic Light Scattering Data for Nanocrystalline Suspension of 1c.

Unimodal Results Summary

Rept#.	Mean (nm)	Std.Dev (nm)	Baseline Error	P.I.	Counts/s	Diff.Coef (m^2/s)	Overflow
Rept.1	187.5	88.7	0.01%	1.064	9.74e+04	2.41e-12	0
Rept.2	203.3	89.7	0.55%	0.439	1.02e+05	2.23e-12	0
Rept.3	221.9	95.0	0.35%	0.343	1.04e+05	2.04e-12	4
Average	204.2	91.12		0.615			

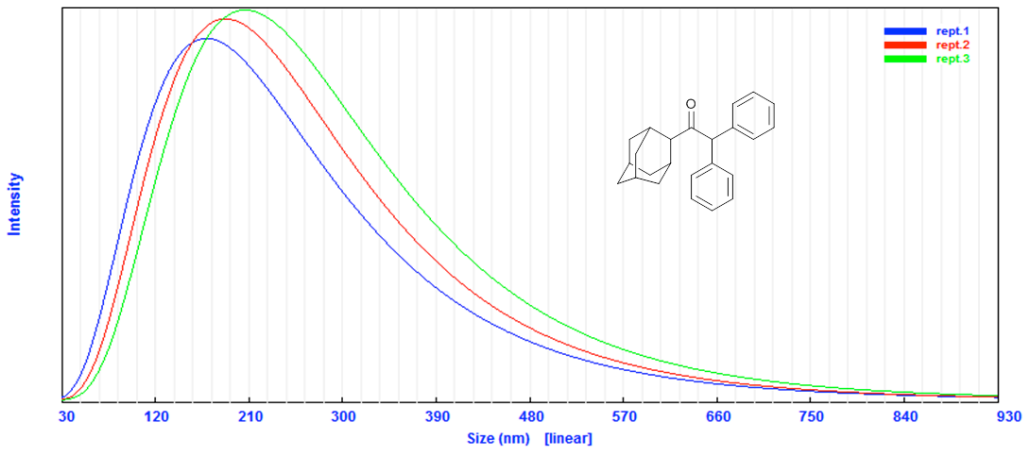

Figure S32. Dynamic Light Scattering Data for Nanocrystalline Suspension of 1d.

Unimodal Results Summary

Rept#.	Mean (nm)	Std.Dev (nm)	Baseline Error	P.I.	Counts/s	Diff.Coef (m^2/s)	Overflow
Rept.1	206.2	99.0	0.64%	1.484	3.49e+04	2.19e-12	0
Rept.2	220.4	106.9	0.24%	1.995	3.45e+04	2.05e-12	0
Rept.3	243.9	113.3	0.12%	0.786	3.48e+04	1.86e-12	0
Average	223.5	106.39		1.422			

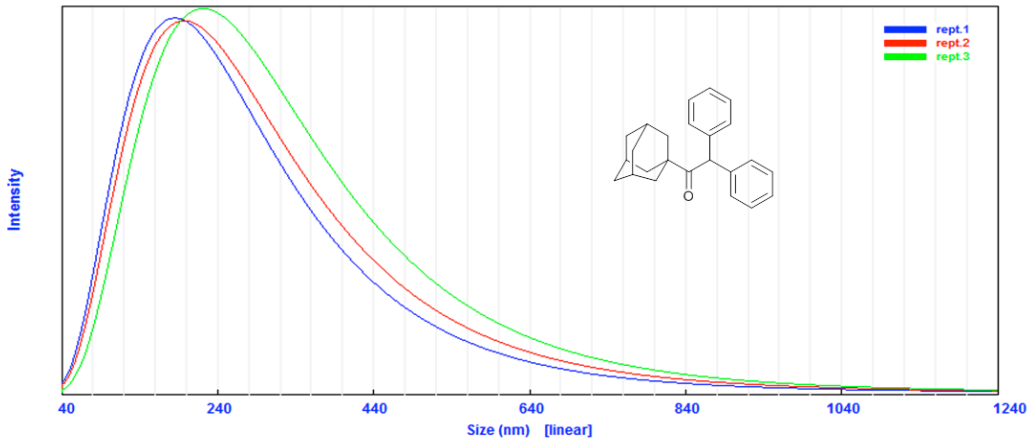

Figure S33. Crystal structure of 1d with thermal ellipsoids drawn at the 50% probability level.

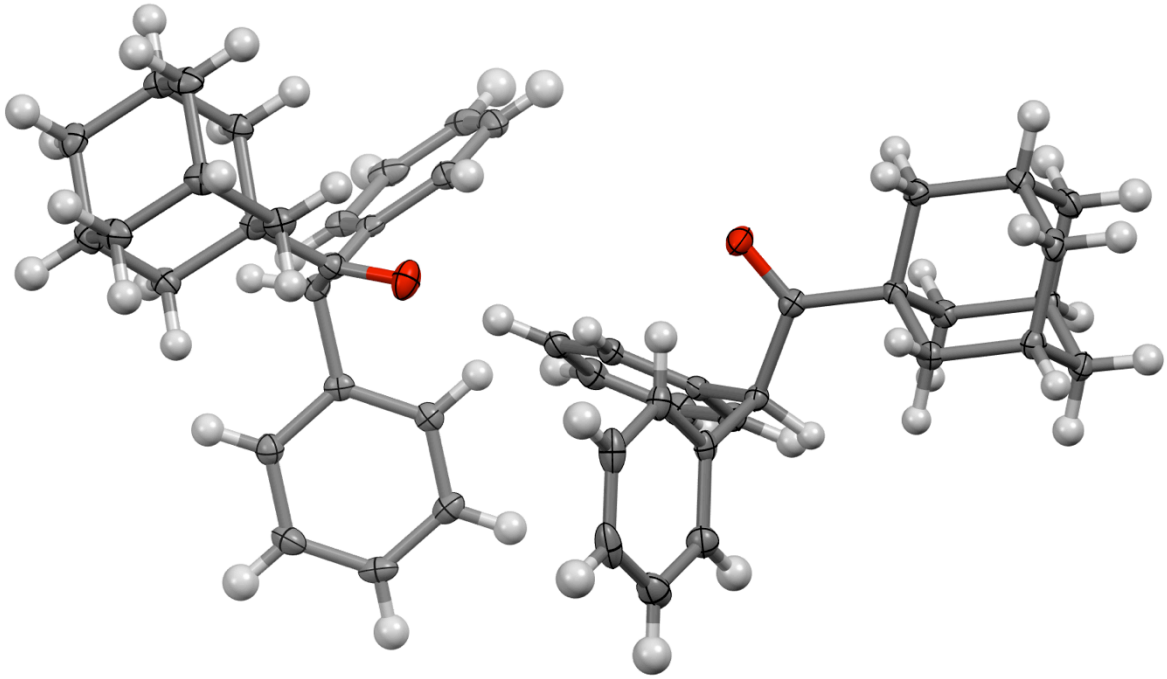

Space Group	$P2_1/c$
a (Å)	11.1701
b (Å)	13.5652
c (Å)	23.6838
α (°)	90
β(°)	91.020
γ(°)	90
Z	8
Volume (Å^3)	3588.11
GoF	1.022
R (%)	4.11

Rw (%)	10.24

References

(1) Adams, R.; Ulich, L. H. The Use of Oxalyl Chloride and Bromide for Producing Acid Chlorides, Acid Bromides or Acid Anhydrides. III. *J. Am. Chem. Soc.* **1920**, *42*, 599–611.

(2) Rajca, A.; Tolbert, L. M. Y-Conjugated Dianions. A 13C Nuclear Magnetic Resonance Study. *J. Am. Chem. Soc.* **1988**, *110*, 871–876.